BMC Genomics

RESEARCH

Open Access

Transcriptome analysis reveals age-specific growth characteristics in the rumen of Hanwoo (Korean native cattle) steers

Yejee Park[1†], Sunsik Jang[2†], Han-Ha Chai[1], Ju-Whan Son[1], Dajeong Lim[3] and Woncheoul Park[1*]

Abstract

Background Hanwoo cattle are a Korean breed renowned for their cultural significance and high-quality beef, characterized by low cholesterol and a high unsaturated fat ratio. Their growth is divided into a growing stage focused on development and a fattening stage for marbling. Proper feed management, considering genetic and environmental factors, is vital for maximizing growth potential. The rumen plays a crucial role in digestion and gene expression regulation, with rumen fermentation being central to nutrient absorption and cattle health. In this study, we conduct a transcriptome analysis of the rumen at eight timepoints. Our goal is to identify genetic factors that influence the growth of Hanwoo steers to enhance our understanding of the rumen's functions during Hanwoo growth.

Results In the RNA-sequencing analysis of Hanwoo steer rumen, differential gene expression was examined over eight timepoints, highlighting significant genetic changes, particularly between 12 and 26 months. The results of a weighted gene co-expression network analysis were identified and organized into three modules: turquoise, blue, and yellow. The turquoise module, linked to immune response, showed significantly down-regulation in genes at 30 months. The blue module, associated with steroid metabolism, was notably up-regulated at 26 months. The yellow module's genes showed a consistent increase in expression with growth. These modules and their functional annotations provide a deeper understanding of the biological processes during Hanwoo growth, highlighting the intricate relationship between gene expression and cattle development.

Conclusions The growth stages of Hanwoo steers were explored in our investigation utilizing rumen transcriptome data. The rumen plays a critical role in their development, particularly during the growing and fattening stages. Proper feed management, considering the rumen's function, is essential for optimal growth. Transcriptome analysis helps identify genes associated with growth and provides insights for cattle breeding and management practices. Understanding the complex connection between gene expression and Hanwoo development is essential for maximizing productivity and health.

[†]Yejee Park and Sunsik Jang contributed equally to this work.

*Correspondence:
Woncheoul Park
wcpark1982@korea.kr

Full list of author information is available at the end of the article

Keywords Hanwoo, Korean native cattle, Growth stage, Transcriptome analysis, Differentially expressed gene (DEG), Gene co-expression network (GCN), Weighted gene co-expression network analysis (WGCNA)

Background

Hanwoo, native beef cattle breed in Korea, has a long-standing history of coexistence with the Korean people, profoundly influencing both agricultural technology and cultural traditions. Esteemed not only domestically but also internationally, Hanwoo is distinguished from other breeds on the basis of its exceptional attributes, including a low cholesterol content, a favorable unsaturated to saturated fatty acids ratio, and superior intramuscular fat content, which is particularly prized for grilling applications [1]. Notably, Hanwoo steers are preferred for grilling owing to their superior intramuscular fat content and meat quality compared to heifers [2].

The growth trajectory of Hanwoo is typically delineated into two principal stages: the growing stage, encompassing the period until approximately 14 months of age, during which skeletal, organ, and muscular development predominates, and the subsequent fattening stage, extending until slaughter, marked by the accumulation of intramuscular fat, ultimately yielding high-quality meat [3]. If we were to divide the growth stages in more detail, they can be categorized as follows: the growing stage from 6 to 14 months, the early fattening stage from 15 to 22 months, and the late fattening stage from 23 to 30 months. Across these stages, effective management strategies are essential. In particular, careful consideration of feed composition—including the type of roughage, concentrated feed, and supplementary feed—is crucial to ensure optimal growth and development [4]. While roughage feed rich in fiber is crucial for tissue building during the growing stage, concentrated feed assumes precedence in the fattening stage to facilitate fat deposition [5].

The high-quality production of Hanwoo beef relies on excellent growth characteristics, including variations in body weight, fat content, muscle mass, and skeletal mass, which fluctuate monthly. Genetic and environmental factors interact, and to maximize the growth potential of Hanwoo, both must be considered. Genetic factors determine not only growth characteristics such as loin cross-sectional area, marbling score, and carcass weight but also reproduction, lifespan, health, and productivity [6, 7]. Environmental factors also influence growth characteristics through factors such as feed, rearing methods, climate, and diseases.

As ruminants, cows primarily consume high-fiber foods including grass and hay, underscoring the vital role of their digestive organ, the rumen. Within the rumen, fermentation is pivotal for the breakdown and digestion of various feeds, facilitating the absorption of essential nutrients critical for cattle health and productivity. This fermentation process, central to cattle digestion, holds particular significance in Hanwoo, as it is a key regulator of gene expression [8]. Inside the rumen, a complex ecosystem is constructed where microorganisms decompose dietary fiber, generating organic acids, gases, and proteins that profoundly influence cattle health and productivity [9]. The composition and abundance of rumen microorganisms, alongside the efficiency of fermentation and the resultant products, exert significant impacts on various physiological aspects of cattle, including energy metabolism, growth hormone secretion, and gene expression. Consequently, scrutinizing changes in rumen characteristics becomes imperative to gain insight into the gene expression and growth characteristics of Hanwoo. Understanding the intricacies of rumen fermentation and its implications on Hanwoo physiology is essential for optimizing cattle health and productivity. Several genes have been suggested to play critical roles in rumen development and cattle growth. For instance, IGF1 and GHR are key regulators of somatic growth and muscle development [10], while PPARG and SCD are involved in lipid metabolism and intramuscular fat deposition during the fattening stage [11, 12]. These candidate genes provide important biological context when interpreting transcriptomic changes across growth stages in Hanwoo cattle.

In this study, we investigate the monthly growth characteristics of Hanwoo steers by utilizing transcriptome analysis of the rumen. Transcriptome analysis entails assessing mRNA expression levels, which provides insights into the genes that govern various functions associated with growth. Through DEG analysis, we aim to underscore the alterations in rumen function. Additionally, by constructing co-expression gene networks, we seek to elucidate metabolic changes and regulatory mechanisms within the rumen. Based on these results, we aim to discover genetic factors that can improve the growth characteristics of Korean beef cattle, thereby paving the way for advancements in breeding and management.

Materials and methods

Study design and RNA sequencing

The study design is depicted in Fig. 1a. A total of sixty-one Hanwoo steers were utilized in this study, slaughtered at eight different timepoints: 6 months (6 M; $n = 6$), 10 months (10 M; $n = 9$), 12 months (12 M; $n = 10$), 14 months (14 M; $n = 8$), 18 months (18 M; $n = 8$), 22 months (22 M; $n = 6$), 26 months (26 M; $n = 8$), and 30 months

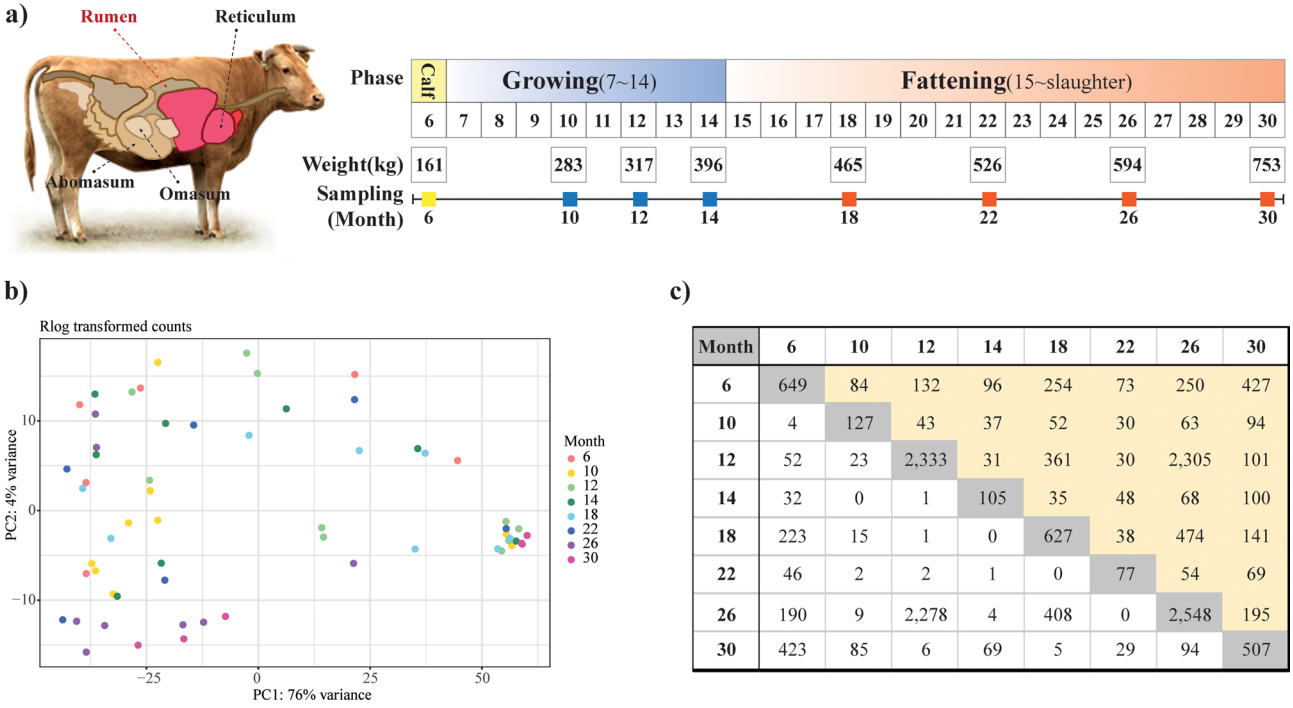

Month	6	10	12	14	18	22	26	30
6	649	84	132	96	254	73	250	427
10	4	127	43	37	52	30	63	94
12	52	23	2,333	31	361	30	2,305	101
14	32	0	1	105	35	48	68	100
18	223	15	1	0	627	38	474	141
22	46	2	2	1	0	77	54	69
26	190	9	2,278	4	408	0	2,548	195
30	423	85	6	69	5	29	94	507

Fig. 1 (**a**) Experimental design of the study. A schematic diagram depicting the experimental design conducted in the rumen of Hanwoo steer across eight timepoints (6, 10, 12, 14, 18, 22, 26, and 30 month). The average weight for each timepoint is shown. (**b**) PCA plot for all samples of eight timepoints. (**c**) Number of DEGs by timepoints (white), sum of DEGs (gray), and number of duplicated DEGs (yellow)

(30 M; $n = 6$). The reason for selecting into eight timepoints was to examine comprehensively, throughout 6 to 30 months (in 4-month intervals), how the three growth stages of Hanwoo (growing stage, early fattening stage, and late fattening stage) and the changes in feed provided at each stage affect the rumen. In particular, as growth accelerates toward the latter part of the growing stage (6 to 14 months), measurements were taken at 2-month intervals. These 61 Hanwoo steers were raised at the Hanwoo Research Institute within the National Institute of Animal Science, located in Daegwallyeong-myeon, Pyeongchang-gun, Gangwon-do, Republic of Korea (average temperature: 7.1 °C, maximum: 12.2 °C, minimum: 2.3 °C). They were born and bred at this farm. Additionally, the feed composition for each stage of growth (Growing stage, early fattening stage, and fattening stage) is provided in Supplementary Table 8 (Table S8). Rumen samples were collected from each steer. Total RNA was extracted from ~20 mg tissue using QIAzol® Lysis Reagent (Qiagen, Cat. No. 79306) and the RNeasy® Mini Kit (Qiagen, Cat. No. 74106). Samples were homogenized in 750 µL QIAzol with a 3 mm stainless steel bead using a TissueLyser at 20 Hz for 2 min. Following the addition of 150 µL chloroform, samples were vortexed for 15 s, incubated at room temperature for 2–3 min, and centrifuged at 12,000 × g for 15 min at 4 °C. The aqueous phase was mixed with 350 µL RLT buffer and 250 µL isopropanol, then loaded onto RNeasy spin columns. RNA purification involved vacuum-assisted binding and washing steps, including DNase I treatment (80 µL; Qiagen, Cat. No. 79254) for 5 min at room temperature. Columns were washed with Buffer RW1 and Buffer RPE, centrifuged to dry, and RNA was eluted in 50 µL RNase-free water. Extracted RNA was stored at − 80 °C until use. Total RNA concentration was measured using the Quant-iT™ RiboGreen RNA Assay Kit (Invitrogen, #R11490), and RNA integrity was assessed with the Agilent TapeStation RNA ScreenTape system (#5067–5576). Only samples with a RNA Integrity Number (RIN) > 7.0 were used for library construction. RNA-seq libraries were prepared using 0.5 µg of total RNA per sample with the TruSeq Stranded Total RNA Library Prep Globin Kit (Illumina, #20020613). Ribosomal RNA was depleted using the Ribo-Zero rRNA Removal Kit (Human/Mouse/Rat Globin), and the remaining RNA was fragmented and reverse-transcribed into cDNA using SuperScript II Reverse Transcriptase (Invitrogen, #18064014) and random primers. Second strand synthesis was performed with DNA Polymerase I, RNase H, and dUTP. The resulting cDNA was end-repaired, A-tailed, and ligated with sequencing adapters, followed by PCR enrichment. Final libraries were quantified using the KAPA Library Quantification Kit (KAPA BIOSYSTEMS, #KK4854) and assessed for quality using the TapeStation D1000 ScreenTape (Agilent, #5067–5582). Indexed libraries were sequenced on the Illumina NovaSeq 6000 platform

(2 × 100 bp paired-end reads) by Macrogen Inc. (Seoul, South Korea).

NGS data preprocessing and DEG identification

The quality of RNA-seq data was checked with FastQC v0.11.9 [13], and the reads were filtered using Trimmomatic v0.36 for low-quality reads and adapter sequences [14]. Filtered reads were mapped against bovine reference (*Bos taurus*; ARS-UCD1.2) with Hisat2 v2.2.1 [15]. GTF *Bos taurus* v103 (Ensembl) was used for exon calculation in each library by subread package v2.0.3 of featureCounts [16].

DEG analysis was performed by pair-wise comparing every timepoints (6 M, 10 M, 12 M, 14 M, 18 M, 22 M, 26 M, and 30 M), respectively. A total of 28 pair-wise comparisons were performed from count data, produced in the previous process. All DEG analyses were performed using DESeq2 v1.24.0 from the R program Bioconductor package [17]. The genes with zero counts across all samples were removed. For PCA, hierarchical clustering, and heatmap analyses, data were normalized using variance stabilizing transformation (VST) and regularized log transformation (RLOG). For differentially expressed gene (DEG) analysis, normalization was performed using DESeq2's median of ratios method that counts divided by sample-specific size factors determined by median ratio of gene counts relative to geometric mean per gene. The threshold for DEG was applied employing the adjusted *p*-value using the Benjamini-Hochberg correction with a false discovery rate of < 0.05 and the absolute log2 fold change (FC) ≥ 1 [18].

Gene Co-Expression Network (GCN) analysis

Weighted gene co-expression network analysis (WGCNA) was selected for the GCN analysis. DEGs with an absolute $\log_2$ fold change (FC) ≥ 3 were used for WGCNA input as converted read counts. Eight timepoints were used as traits and the Pearson method was used to evaluate the correlation. In our analysis, we applied the WGCNA::blockwiseModules() function using the following settings: soft-threshold power = 7, TOMType = "unsigned", minimumModuleSize = 10, reassignThreshold = 0, and mergeCutHeight = 0.25. In addition, the hard threshold 0.05 was adjusted in each module for filtering [19]. Afterwards, in order to select relevant genes in the network, the network was reconstructed with genes with an edge weight of 0.3 or more.

Results of WGCNA were visualized using Cytoscape v3.10.1 software and genes were shown as nodes and the correlations between genes calculated through WGCNA were viewed as edge weights in the network.

Functional analysis and candidate hub gene

The functions of the network analysis were annotated using Database for Annotation, Visualization and Integrated Discovery (DAVID 2021, https://david.ncifcrf.gov/) [20]. Kyoto Encyclopedia of Genes and Genomes (KEGG) pathways and gene ontology (GO) terms were used for DEG functional analyses of WGCNA results.

Significant gene candidates were determined considering the number of edges, the possibility of being a hub gene indicated by the number of edges, and the significance according to expression levels within the genes in the WGCNA modules.

Results

Overview of RNA-seq data processing and DEG analysis

In this study, we used rumen sample of Hanwoo steer from 64 individuals. About 2.2 billion paired-end sequence reads were generated with an average of 36.7 million reads per sample. The clean reads that passed the quality trimming process average 36.2 million with an average trimming rate of 1.17 ± 1.32%(average ± standard deviation(SD)). After trimming, clean reads were aligned with an average unique mapping rate of 83.62 ± 1.32%(average ± SD)% and an average overall mapping rate of 94.67 ± 2.5%(average ± SD)% to bovine reference genome ARS-UCD1.2 (Table S1). The expression values of 61 samples from eight timepoints are presented in a PCA plot representing data characteristics through dimensionality reduction (Fig. 1b).

Figure 1c illustrates the number of DEGs identified across different age groups. The 26 M group showed the highest number with 2,548 DEGs, followed by the 12 M group with 2,333 DEGs. A total of 2,278 DEGs were detected in the comparison between 12 M and 26 M, resulting in 2,305 overlapping DEGs between these two groups—the highest among all pairwise comparisons. The second highest overlap was observed between 18 M and 26 M, with 474 shared DEGs. Between 12 M and 26 M, axon guidance turned out to be the significant biological term both between 12 M and 26 M, and 18 M and 26 M, and the term was composed with down-regulated DEGs. Afterwards, regulation of I-kappaB kinase/NF-kappaB signaling appeared as the most significant biological term between 18 M and 26 M.

CGN analysis and functional annotations of WGCNA modules

501 DEGs with stricter threshold of an absolute $\log_2$ fold change (FC) ≥ 3 were once more filtered to create GCN using WGCNA (Table S2). A prior WGCNA result was composed of six modules (Fig. 2b). Among the six modules(WGCNA settings: soft-threshold power = 7, TOMType = "unsigned", minimumModuleSize = 10, reassignThreshold = 0, mergeCutHeight = 0.25, and hard

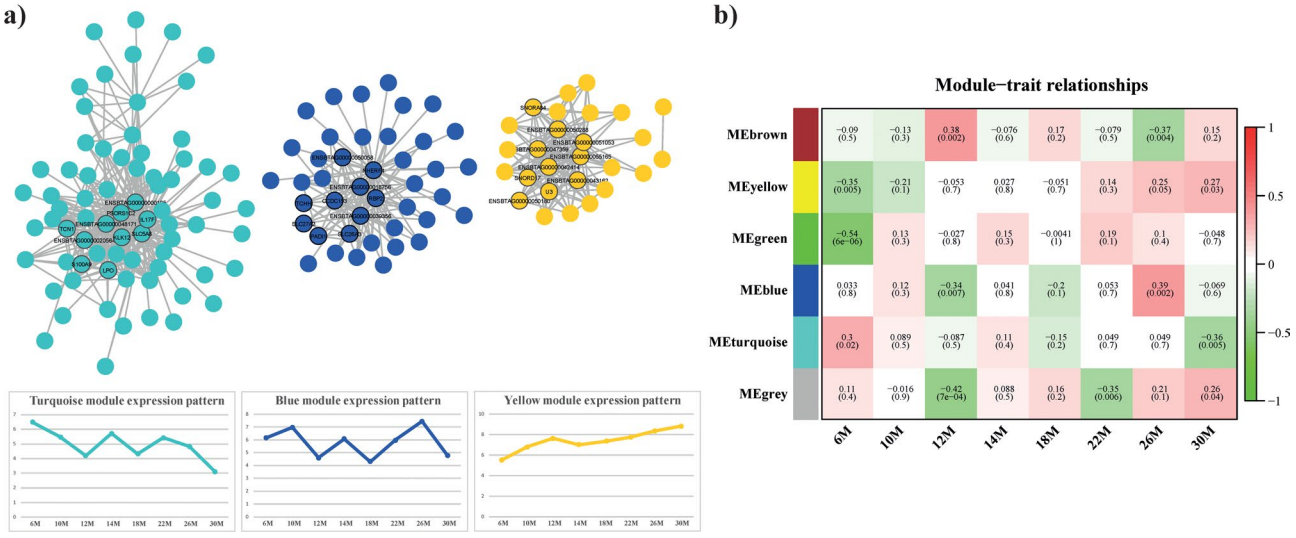

Fig. 2 (**a**) WGCNA network and expression patterns of three modules (turquoise, blue, and yellow). Nodes are composed by DEGs with an absolute foldchange value of 3 or more. Only nodes connected by edges with a weight value of 0.3 or higher are displayed. Top 10 candidate gene name of each module are displayed. (**b**) Module-trait correlation heatmap. The correlation between each module and 8 timepoints is shown with *p*-value

threshold = 0.05), 144 DEGs with an edge weight of 0.3 or more were filtered once more and composed the final network (Fig. 2a). As a result, three modules were remained (turquoise: 73 nodes, blue: 42 nodes, yellow: 27 nodes).

The largest module in this study, referred to as the turquoise module, comprises 73 nodes and 313 edges. The functional analysis of this module reveals key terms in the Gene Ontology's biological process, including neutrophil chemotaxis and positive regulation of cytokine production involved in the inflammatory response (Fig. 3a). Similarly, the KEGG pathway analysis highlights the prominence of immune-related pathways, specifically the IL-17 signaling pathway and cytokine-cytokine receptor interaction (Fig. 3c). The number of edges was calculated for all genes within the turquoise module, and the top 10 genes are presented in Table 1. Among these, four genes (*LPO*, *SLC5A8*, *S100A9*, and *TCN1*) stood out as candidate hub genes due to their high number of edges, stage-specific expression, differential expression, and immune-related functions aligned with the module's characteristics. Notably, these genes were found to be particularly down-regulated at 30 months of age.

The second largest module of the WGCNA results, the blue module, is composed of 42 nodes and 126 edges. The functional analysis of this module highlighted key BP terms, notably the doxorubicin metabolic process and fatty acid transport (Fig. 3c). The KEGG pathway analysis further revealed the prominence of several pathways, including drug metabolism– cytochrome P450, metabolism of xenobiotics by cytochrome P450, inositol phosphate metabolism, retinol metabolism, and steroid hormone biosynthesis (Fig. 3d). Candidate hub genes for this module were identified as *RBP2*, *NHERF4*, *SLC26A3*, *SLC27A2*, and ENSBTAG00000039356. The expression pattern of the blue module was not consistent throughout the growth period, but it was most significantly up-regulated at 26 months.

The final WGCNA module, the yellow module, is composed of 27 nodes and 140 edges. From the result of the functional analysis, this module was not included in a specific pathway. The gene constituting this module exhibited an increasing trend in expression with growth.

Discussion

In this study, we investigated the growth stages of Hanwoo steer, dividing them into eight time-series, and analyzed gene expression patterns related to growth using rumen transcriptome data. The rumen plays a critical role at each growth stage in Hanwoo. Specifically, the fermentation process by microorganisms within the rumen is of significant importance, as it involves breaking down feed and producing nutrients [21]. The control of ruminal acidity is crucial, as it provides an optimal environment for this microbial ecosystem. Consequently, this is essential for the growth, productivity, and health of Hanwoo. The growth stages of Hanwoo are primarily divided into the rearing stage and the fattening stage, with this division typically occurring at around 14 months of age. During the rearing stage, the focus is on the growth and development of the cattle, and leveraging the rumen's function to its fullest potential is crucial. In this stage, roughage feed, which is typically rich in fiber such as grass, hay, and silage, is needed to support the development of the rumen and ensure balanced nutrition. This diet helps in maximizing the rumen's efficiency

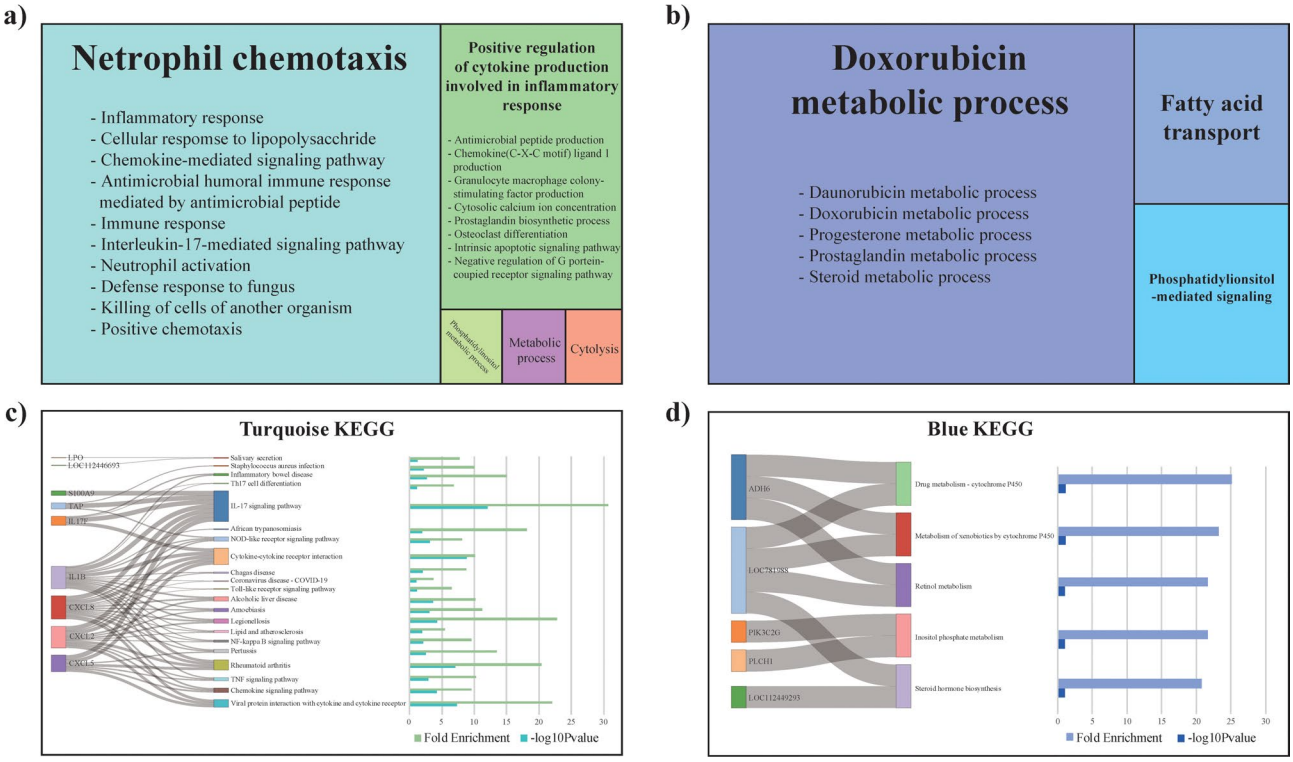

Fig. 3 Functional analysis results. (**a**) The representative and descriptive terms from the GO BP results of the turquoise module are presented. (**b**) The representative and descriptive terms from the GO BP results of the blue module are presented. (**c**) KEGG pathway results of turquoise module were visualized as bar graphs including fold enrichment and $-\log_{10}(p\text{-value})$. (**d**) KEGG pathway results of blue module were visualized as bar graphs including fold enrichment and $-\log_{10}(p\text{-value})$

for better digestion and nutrient absorption in later stages, promoting healthy growth of Hanwoo. During the fattening stage of Hanwoo, concentrated feed is primarily fed instead of roughage feed. The feed in this stage has a high energy density, focusing on optimizing weight gain and meat quality. Concentrated feed continuously supports the growth and contributes to the development of meat characteristics such as marbling [22]. Understanding the growth stages of Hanwoo and appropriately managing the function of the rumen are essential for healthy growth, productivity, and well-being. Transcriptome analysis using RNA-seq can provide insights into the mechanisms of the rumen and help identify genes that significantly change during different growth stage of Hanwoo steer.

Rumen acidity and immune responses through the growth process

Rumen acidity, maintaining a stable pH level of about 5.6 to 5.8, serves as a crucial indicator of cattle health [23]. This acidity significantly impacts the growth and function of microorganisms within the rumen. Specifically, elevated acidity levels can inhibit certain microorganisms, particularly those involved in cellulose breakdown and methane production, potentially compromising fiber digestion and energy production. Conversely, maintaining optimal acidity fosters robust microbial activity, thereby promoting increased fiber degradation and the production of volatile fatty acids (VFAs). These VFAs, generated through fermentation by diverse rumen microorganisms, serve as a vital energy source for cattle. Notably, propionic acid undergoes conversion into glucose in the liver, contributing to energy production and fat synthesis within the body.

In the turquoise module results of WGCNA, *LPO* and *SLC5A8*, considered hub genes, show significantly downregulated expression as Hanwoo grows. *LPO*, a gene associated with the KEGG pathway salivary secretion, encodes the enzyme Lactoperoxidase, which is secreted in saliva and other bodily fluids, contributing to nonspecific fluid immune responses. When transitioning from roughage to concentrate feed, reduced rumination frequency and duration suppress saliva secretion in cattle. Lower expression of *LPO* may also impact the function of salivary glands responsible for saliva production. Saliva acts as a buffer to maintain rumen pH, but reduced secretion results in the accumulation of organic acids from high-nutrient diets, lowering rumen pH from 5.5 to 5.0. This disruption in rumen acidity balance can trigger subacute rumen acidosis (SARA), which is implicated

Table 1 Candidate gene list of three modules. Genes with top 10 number of edge are selected

Module	Candidate gene	#Edge	Expression level							
			6 M	10 M	12 M	14 M	18 M	22 M	26 M	30 M
Turquoise	*SLC5A8*	43	8.79863	7.405719	5.404076	7.522423	6.040697	7.224633	6.877005	3.278463
	ENSBTAG00000000185	36	9.614279	8.446257	6.464829	8.302271	6.493767	8.553656	6.351373	4.646231
	ENSBTAG00000048171	35	12.27628	9.695177	6.852681	11.32645	8.692354	10.86638	9.704314	4.539787
	PSORS1C2	31	7.362203	6.166217	4.286312	5.954387	5.239768	6.481933	4.981247	2.808648
	IL17F	25	8.282685	5.779358	3.938809	6.342225	3.498025	5.657185	5.218373	2.937169
	KLK12	20	6.933009	5.070095	4.395617	6.384025	4.439513	7.165776	5.411065	2.417109
	LPO	19	8.70424	8.387793	6.788237	8.062357	6.316045	8.139178	6.573461	4.118583
	S100A9	15	15.05009	13.65595	10.65488	13.0784	11.29686	13.38196	12.44524	6.718793
	TCN1	15	6.998888	6.23649	3.77969	7.817053	4.986923	6.558801	4.926604	2.954202
	ENSBTAG00000020564	13	9.639412	7.523189	4.065774	10.39003	6.865432	7.675511	5.777105	3.386722
Blue	*RBP2*	27	10.01199	9.696882	7.418318	9.576032	5.992223	9.592235	10.99401	6.002023
	NHERF4	22	9.33302	9.809584	6.543961	9.292665	5.711167	8.737079	9.796566	6.697287
	ENSBTAG00000039356	16	6.92449	7.260121	4.799424	6.818613	4.2355	7.222507	8.126471	4.641059
	ENSBTAG00000018756	14	5.720669	6.270472	4.508988	5.429931	3.52806	5.305524	6.605274	4.05363
	CCDC153	9	7.899008	8.556084	5.309857	7.380313	4.577448	7.136309	8.532687	5.772409
	PADI1	7	4.062364	5.37351	2.079436	3.65022	3.482273	3.95551	6.7783	5.015449
	ENSBTAG00000050058	6	11.87831	12.42465	8.48923	8.800488	8.290755	8.327265	13.1507	8.508881
	SLC27A2	6	4.784789	5.546717	3.672654	4.920731	3.355447	4.937327	6.567251	5.045156
	TCHH	5	9.3847	10.04018	6.187069	6.986331	6.315587	6.104281	10.29379	7.322607
	SLC26A3	5	12.28137	12.59722	8.149106	10.84071	7.242773	11.18417	13.11576	8.10057
Yellow	ENSBTAG00000055165	16	5.851102	6.934004	7.285027	7.08609	6.913771	7.695383	9.309291	8.757692
	ENSBTAG00000051053	15	5.073161	6.514673	7.410047	6.576222	6.664073	7.973333	9.109355	8.674033
	U3	15	8.311636	8.622901	11.51928	9.105007	10.05991	10.144	11.99789	12.32606
	ENSBTAG00000047359	14	4.39335	6.115048	6.992509	5.89895	5.388648	6.808304	7.267227	8.55569
	ENSBTAG00000050288	14	4.700326	5.897152	6.832309	5.609684	6.460362	6.821131	7.822698	8.663347
	SNORD17	11	6.578983	8.9503	9.993376	7.450884	8.489505	10.14559	9.70133	10.61683
	SNORA84	11	4.90606	5.956345	6.026403	5.450718	5.568092	5.6559	6.947627	6.948076
	ENSBTAG00000043162	10	4.921612	6.730455	7.968126	6.47485	6.358343	7.445553	7.533879	8.267649
	ENSBTAG00000042414	10	6.649432	7.340468	8.551107	7.70609	7.754667	8.284703	9.269335	9.471897
	ENSBTAG00000050180	9	11.42412	15.58276	16.49247	14.35375	16.75237	16.71149	16.47244	16.70431

in various digestive disorders including indigestion and diarrhea (Fig. 4.) [24]. Similarly, decreased expression of *SLC5A8* contributes to the onset of SARA by impeding the absorption of short-chain fatty acids (SCFA), a type of VFA, from the rumen [25]. After Hanwoo reach an age of approximately 14 months, there is a gradual increase in the proportion of concentrated feed they are given. When growth has been completed at 30 months, and fattening is finished with a relatively high proportion of concentrated feed, the production and absorption of VFAs decrease in Hanwoo compared to others that are still in their growing and fattening stages.

Also, hub genes that regulated inflammatory responses were selected. *S100A9* (S100 calcium-binding protein A9), one of the S100 family, is a calcium-binding protein that regulates calcium homeostasis [26]. According to previous research, *S100A9* plays a role in various cellular processes such as cell cycle progression and differentiation. This reduces intracellular ROS, but increases cytokine and chemokine secretion that mediates induced inflammation [27, 28]. *TCN1*, which encodes the protein Transcobalamin 1, transports vitamin B12 in the blood to nerve cells, red blood cells, and other tissues [29]. Furthermore, *TCN1* is a significant component of secondary granules in neutrophils and also plays a role in the immune system, potentially regulating the inflammatory response and bolstering defenses against infections [30]. Both *S100A9* and *TCN1* have been shown in studies to influence cell growth, tissue regeneration, and the development of cancer [31, 32]. During early development, individuals primarily rely on innate immunity, the immune system they are born with, since their acquired immune system is not yet fully developed [33]. Acquired immunity, which includes mature B cells and T cells, forms immune memory against specific pathogens and produces antibodies [34]. In fully grown individuals, while innate immunity remains active, the acquired immunity also comes into play. A mature and stable immune system may result in a relatively less active immune response [35]. Consequently, it is considered that Hanwoo at six months of age exhibit a more active immune response compared to those that have

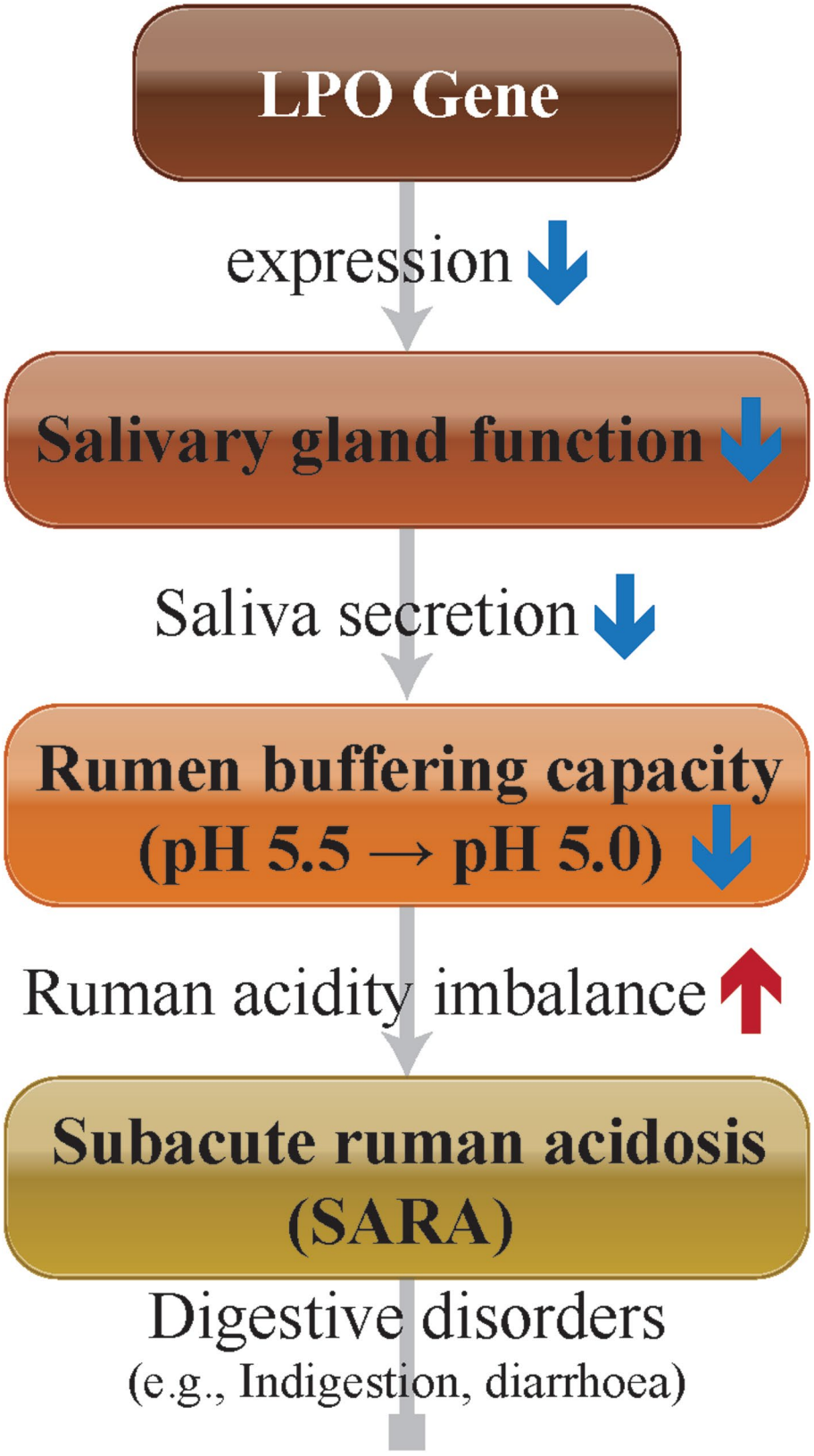

Fig. 4 Schematic diagram showing the potential role of LPO gene in ruman acidity regulation and digestive health

completed growth at 30 months of age. This heightened immune response is associated with increased expression of immune-related hub genes.

The growth process: protein biosynthesis and steroid metabolism

Most of the genes in the yellow module, such as *SNORD17*, are either not well-characterized or are known to be small nucleolar RNAs (snoRNAs), which play critical roles in RNA processing and enhance RNA stability during protein synthesis [36]. These snoRNAs are involved in post-transcriptional modifications of rRNAs, including 2′-O-methylation and pseudouridylation, which are essential for proper ribosomal assembly, translational fidelity, and overall protein biosynthesis [36–38]. These functions become particularly important during periods of elevated anabolic activity, such as tissue development and fattening in beef cattle. Transcriptome analysis in our study showed that the expression of snoRNAs, including *SNORD17*, increased progressively with age in Hanwoo steers, peaking at 30 months, suggesting their involvement in supporting the enhanced translational and metabolic demands during late-stage growth. In particular, *SNORD17* has been shown to interact with nucleophosmin (*NPM1*) and MYB-binding protein 1 A (*MYBBP1A*), leading to suppression of p53 activity, thereby promoting cell cycle progression and inhibiting apoptosis [39, 40]. Although these findings were primarily reported in human disease models such as hepatocellular carcinoma, they underscore the broader regulatory potential of *SNORD17* beyond canonical RNA modification. Taken together, these findings support the hypothesis that snoRNA-mediated regulation may contribute to maintaining cellular homeostasis and promoting tissue-specific growth and metabolic adaptation during the late fattening stage in Hanwoo cattle. Further studies are warranted to clarify the specific biological roles of snoRNAs in bovine development and growth.

The rumen underpins the digestion and absorption process of Hanwoo by breaking down large and complex molecules into smaller, absorbable units. This includes the breakdown of proteins, fats, and carbohydrates into sugars, VFAs, and other simpler molecules. Absorbed nutrients are used as ingredients for tissue, muscle, and bone growth with the help of steroid hormones [41]. The blue module's analysis revealed functions related to metabolism of xenobiotics by cytochrome P450, and the metabolism and biosynthesis of fatty acids and steroids. Among the candidate genes in the blue module, *RBP2* and *NHERF4* are involved in nutrition absorption, which can significantly degrade growth if insufficient. *RBP2* (retinol binding protein 2), a member of the fatty acid-binding protein family, is recognized for its involvement in vitamin A uptake and metabolism [42]. *NHERF4*, which encodes the NHERF family PDZ, negatively regulates the activation mediated by heat-stable enterotoxin [43]. As the previous study shows, *NHERF4* interacts with *SLC26A3*, which is also a candidate gene in the blue module and modulates the luminal fluidity [44]. *SLC27A2* (solute carrier family 27 member 2), which encodes FATP2, plays a pivotal role in lipid biosynthesis and fatty acid degradation [45]. It converts free long-chain fatty acids into fatty acyl-CoA esters [46]. In addition, ENSBTAG00000039356 is related to metabolic process-related BP terms, which are a steroid metabolic process, daunorubicin metabolic process, doxorubicin metabolic process, progesterone metabolic process, and prostaglandin metabolic process. Daunorubicin and doxorubicin have been associated with cytochrome p450 activity, and the majority of cytochrome P450s are involved in the metabolism of steroids, bile acids, fatty acids, eicosanoids, and fat-soluble vitamins [47]. They are also involved in the metabolism of drugs and other xenobiotic chemicals [48]. The expression of hub genes from the blue module undergoes a dramatic increase at 26 months of age during the late fattening stage, compared to 12 to 18 months of age in the growing and early fattening stage. Steroid hormone usage increases skeletal muscle metabolism, leading to muscle hypertrophy and enhanced physical function [49]. Muscle growth and metabolism are notably more active in Hanwoo during the late fattening stage compared to the early fattening stage, with 26 months of age considered the peak of growth.

Conclusions

Based on our study investigating monthly growth characteristics of Hanwoo steers via a rumen transcriptome analysis, we have gained insights into genetic factors influencing growth in Hanwoo. These insights shed light on how rumen physiology, gene expression, and growth dynamics intersect. Our findings underscore the rumen's vital role in facilitating growth and nutrient utilization across developmental stages, with notable changes in acidity and key gene expression impacting growth performance and health. We identified candidate genes linked to processes such as the immune response, steroid metabolism, and nutrient absorption, revealing molecular mechanisms behind Hanwoo growth. Differential gene expression across growth stages highlights the dynamic nature of rumen function and its impact on Hanwoo growth performance. These findings contribute to a deeper understanding of the genetic factors underlying growth in Hanwoo steers.

Abbreviations

DEG	Differentially expressed gene
GCN	Gene co-expression network
WGCNA	Weighted gene co-expression network analysis

KEGG	Kyoto encyclopedia of genes and genomes
GO	Gene ontology
BP	Biological process

Supplementary Information

The online version contains supplementary material available at https://doi.org/10.1186/s12864-025-11712-9.

Supplementary Material 1

Supplementary Material 2

Acknowledgements
Not applicable.

Author contributions
Y.P. collected the samples, analyzed the data and drafted the manuscript. J-H.S. and L.D. collected the samples. S.J. provided sample and phenotype information. H-H.C. provided comments on the analysis and the manuscript. W.P. collected the samples, revised the manuscript and supervised the study. All authors read and approved the final manuscript.

Funding
The author(s) declare financial support was received for the research, authorship, and/or publication of this article. This study was carried out with the support of 2020 the RDA Fellowship Program of the NIAS and Cooperative Research Program for Agriculture Science and Technology Development (Project No. PJ01492004, "Determination of growing performance, tissue physiology and meat quality change in Hanwoo steers"), Rural Development Administration, Republic of Korea.

Data availability
The RNA sequencing data were freely deposited at the National Center for Biotechnology Information (NCBI) Gene Expression Omnibus (GEO) database under accession number GSE267733.

Declarations

Ethics approval and consent to participate
This study was approved by the local committees and the research ethics committees of the National Institute of Animal Science, Republic of Korea. The experimental protocols were approved by the Committee on the Ethics of Animal Experiments of the National Institute of Animal Science (Permit Number: NIAS2015-776).

Consent for publication
Not applicable.

Competing interests
The authors declare no competing interests.

Author details
[1]Animal Genomics and Bioinformatics Division, National Institute of Animal Science, RDA, Wanju 55365, Republic of Korea
[2]Hanwoo Research Institute, National Institute of Animal Science, RDA, Pyeongchang 25342, Republic of Korea
[3]Department of Animal Resources Science, College of Agriculture and Life Science, Chungnam National University, Daejeon 34134, Republic of Korea

Received: 30 May 2024 / Accepted: 14 May 2025
Published online: 26 May 2025

References

1. Choi C-B, et al. Comparison of cholesterol contents and fatty acid composition in M. longissimus of Hanwoo, Angus and Wagyu crossbred steers. J Anim Sci Technol. 2008;50(4):519–26.
2. Lee S-M, et al. Comparative studies among bull, steer and heifer on growth performance, blood composition and carcass characteristics according to fattening phase in Hanwoo. Korean J Org Agric. 2016;24(4):931–44.
3. Cabezas A, et al. Effect of the inclusion of rumen-protected amino acids in the diet of growing beef cattle on animal performance and meat quality. Front Anim Sci. 2023;4:1269775.
4. Santra A, Karim S. Effect of dietary roughage and concentrate ratio on nutrient utilization and performance of ruminant animals. Anim Nutr Feed Technol. 2009;9(2):113–35.
5. Pethick DW, Harper GS, Oddy VH. Growth, development and nutritional manipulation of marbling in cattle: a review. Aust J Exp Agric. 2004;44(7):705–15.
6. Lee S-H, et al. Hanwoo cattle: origin, domestication, breeding strategies and genomic selection. J Anim Sci Technol. 2014;56(1):1–8.
7. Seo D, et al. Long-term artificial selection of Hanwoo (Korean) cattle left genetic signatures for the breeding traits and has altered the genomic structure. Sci Rep. 2022;12(1):6438.
8. Cho Y, et al. Study on the optimum range of weight-age data for Estimation of growth curve parameters of Hanwoo. J Anim Sci Technol. 2002;44(2):165–70.
9. Grant RJ, Dann HM. Biological importance of rumination and its use on-farm. New York, NY, USA: Agricultural Research Institue Chazy; 2015.
10. Curi RA, et al. Association between IGF-I, IGF-IR and GHRH gene polymorphisms and growth and carcass traits in beef cattle. Livest Prod Sci. 2005;94(3):159–67.
11. Goszczynski DE, et al. Genetic characterisation of PPARG, CEBPA and RXRA, and their influence on meat quality traits in cattle. J Anim Sci Technol. 2016;58:1–9.
12. Mannen H. Genes associated with fatty acid composition of beef. Food Sci Technol Res. 2012;18(1):1–6.
13. Andrews S. FastQC: A quality control application for high throughput sequence data. Babraham Institute; 2012.
14. Bolger AM, Lohse M, Usadel B. Trimmomatic: a flexible trimmer for illumina sequence data. Bioinformatics. 2014;30(15):2114–20.
15. Kim D, et al. Graph-based genome alignment and genotyping with HISAT2 and HISAT-genotype. Nat Biotechnol. 2019;37(8):907–15.
16. Liao Y, Smyth GK, Shi W. FeatureCounts: an efficient general purpose program for assigning sequence reads to genomic features. Bioinformatics. 2014;30(7):923–30.
17. Love MI, Huber W, Anders S. Moderated Estimation of fold change and dispersion for RNA-seq data with DESeq2. Genome Biol. 2014;15:1–21.
18. Benjamini Y, Hochberg Y. Controlling the false discovery rate: a practical and powerful approach to multiple testing. J Roy Stat Soc: Ser B (Methodol). 1995;57(1):289–300.
19. Langfelder P, Horvath S. WGCNA: an R package for weighted correlation network analysis. BMC Bioinformatics. 2008;9:1–13.
20. Dennis G, et al. DAVID: database for annotation, visualization, and integrated discovery. Genome Biol. 2003;4(9):1–11.
21. Um K-H, Park B-K. Study on the rumen fermentation, growth performance and carcass characteristics according to the supplementation of lupin flake in Hanwoo steers. J Anim Sci Technol. 2022;64(6):1077.
22. Shin K, et al. Feed intake evaluation of Korean cattle (Hanwoo) fed diets containing different levels of compound fattening periods. J Anim Sci Technol. 2002;44(1):95–104.
23. Nordlund KV, Garrett EF. *Rumenocentesis: a technique for collecting rumen fluid for the diagnosis of subacute rumen acidosis in dairy herds.* The bovine practitioner, 1994: pp. 109–112.
24. Kleen J, et al. Subacute ruminal acidosis (SARA): a review. J Vet Med Ser A. 2003;50(8):406–14.
25. Zhao C, et al. Potential role of SLC5A8 expression in the etiology of subacute ruminal acidosis. Front Veterinary Sci. 2020;7:394.
26. Zimmer D, et al. *S100-mediated signal transduction in the nervous system and neurological diseases.* Cellular and molecular biology. France). 2005;51(2):201–14. (Noisy-le-Grand.
27. Shepherd C, et al. Inflammatory S100A9 and S100A12 proteins in Alzheimer's disease. Neurobiol Aging. 2006;27(11):1554–63.
28. Nacken W, et al. S100A9/S100A8: myeloid representatives of the S100 protein family as prominent players in innate immunity. Microsc Res Tech. 2003;60(6):569–80.
29. Surendran S, et al. An update on vitamin B12-related gene polymorphisms and B12 status. Genes Nutr. 2018;13:1–35.

30. Campos C, et al. Intramammary infusion of lipopolysaccharide promotes inflammation and alters endometrial gene expression in lactating Holstein cows. J Dairy Sci. 2018;101(11):10440–55.
31. Gebhardt C, et al. S100A8 and S100A9 in inflammation and cancer. Biochem Pharmacol. 2006;72(11):1622–31.
32. Wang Y et al. Transcobalamin I: a novel prognostic biomarker of neoadjuvant chemotherapy in locally advanced hypopharyngeal squamous cell cancers. OncoTargets Therapy, 2018: pp. 4253–61.
33. Horan MA, Ashcroft GS. Ageing, defence mechanisms and the immune system. Age Ageing. 1997;26(suppl4):15–9.
34. Akira S, Takeda K, Kaisho T. Toll-like receptors: critical proteins linking innate and acquired immunity. Nat Immunol. 2001;2(8):675–80.
35. Kim MK, Kim J. Properties of immature and mature dendritic cells: phenotype, morphology, phagocytosis, and migration. RSC Adv. 2019;9(20):11230–8.
36. Fujita T, et al. Identification of non-coding RNAs associated with telomeres using a combination of enchip and RNA sequencing. PLoS ONE. 2015;10(4):e0123387.
37. Frye M, et al. RNA modifications modulate gene expression during development. Science. 2018;361(6409):1346–9.
38. Cui J, et al. SNORD17-mediated KAT6B mRNA 2′-O-methylation regulates vasculogenic mimicry in glioblastoma cells. Cell Biol Toxicol. 2023;39(6):2841–60.
39. Liang J, et al. Non-coding small nucleolar RNA SNORD17 promotes the progression of hepatocellular carcinoma through a positive feedback loop upon p53 inactivation. Cell Death Differ. 2022;29(5):988–1003.
40. Zacchini F, et al. How snornas can contribute to cancer at multiple levels. NAR cancer. 2024;6(1):zcae005.
41. Thornton KJ. *Triennial growth symposium: The nutrition of muscle growth: Impacts of nutrition on the proliferation and differentiation of satellite cells in livestock species.* Journal of Animal Science, 2019. 97(5): pp. 2258–2269.
42. Blaner WS, et al. Retinol-binding protein 2 (RBP2): biology and pathobiology. Crit Rev Biochem Mol Biol. 2020;55(2):197–218.
43. Scott RO, Thelin WR, Milgram SL. A novel PDZ protein regulates the activity of Guanylyl cyclase C, the heat-stable enterotoxin receptor. J Biol Chem. 2002;277(25):22934–41.
44. Lee JH, et al. Regulation of SLC26A3 activity by NHERF4 PDZ-mediated interaction. Cell Signal. 2012;24(9):1821–30.
45. Falcon A, et al. FATP2 is a hepatic fatty acid transporter and peroxisomal very long-chain acyl-CoA synthetase. Am J Physiology-Endocrinology Metabolism. 2010;299(3):E384–93.
46. Korbecki J, et al. Reduced expression of Very-Long-Chain Acyl-CoA synthetases SLC27A4 and SLC27A6 in the glioblastoma tumor compared to the peritumoral area. Brain Sci. 2023;13(5):771.
47. Schroterova L, et al. The effect of new lipophilic chelators on the activities of cytosolic reductases and P450 cytochromes involved in the metabolism of anthracycline antibiotics: studies in vitro. Physiol Res. 2004;53(6):683–91.
48. Guengerich FP. Cytochromes P450, drugs, and diseases. Mol Interv. 2003;3(4):194.
49. Kim YJ, et al. The role of sex steroid hormones in the pathophysiology and treatment of sarcopenia. Osteoporos Sarcopenia. 2016;2(3):140–55.

Publisher's note